Thermolysis of Orthonovolaks. II. Phenol–Formaldehyde and α-Naphthol–Formaldehyde Resins

M. S. CHETAN,[1] R. S. GHADAGE,[2] C. R. RAJAN,[2] V. G. GUNJIKAR,[2] and S. PONRATHNAM[2,*]

[1]Department of Plastics Engineering, University of Lowell, Lowell, Massachusetts 01854; [2]Polymer Science and Engineering Group, Chemical Engineering Division, National Chemical Laboratory, PUNE-411 008, India

SYNOPSIS

A series of α-naphthol–formaldehyde orthonovolak resins were synthesized by altering the mol ratios of α-naphthol and formaldehyde involved in the condensation reaction. Oxalic acid was used as the catalyst. The softening temperatures and thermal degradation behavior of these resins are presented. Thermal degradation kinetics of these resins were investigated by applying nonisothermal integral methods of Coats–Redfern and Horowitz–Metzger. The dynamic thermogravimetric experiments were conducted in air to obtain differential thermogravimetric (DTG) plots. The ratio of the partial integrated area at temperature T to the total area was used to estimate the fractional degradation in the analysis. Degradation proceeded in two stages. The second stage was the predominant one. The thermal degradation profile and activation energies in this stage are discussed in relation to orthonovolaks of similar composition based on phenol–formaldehyde. © 1993 John Wiley & Sons, Inc.

INTRODUCTION

Phenolic resins are perhaps the first synthetic resins to have acquired a significant commercial success. This is due to design flexibility to make resins of widely varying properties by altering the catalyst and the relative mol ratios of phenol to formaldehyde as well as using substituted phenols and other aldehydes. These resins have found a significant role, away from commodity applications, in highly specialized resists formulations used in microelectronics. The orthonovolaks based on phenol–formaldehyde (PF) as well as on substituted phenols form the major constituent in positive photoresist formulations used in optical lithography.[1-3] Unlike novolaks and resoles, the orthonovolaks, formed by substitution exclusively at the two positions *ortho* to hydroxyl group through weak acid catalysis, consist of permanently fusible linear structures. Properties of special significance in microelectronic applications are the enhanced softening and degradation temperatures. Here, the resin is used in combination with a number of low molecular mass compounds such as sensitizers and antihalation agents. This should prevent the crystallization of these by forming an uniform film. Recently, α-naphthol–formaldehyde orthonovolaks have become resins of choice in these applications. This study highlights the thermal properties of these resins in relation to this application. The enhanced softening temperatures translates into a decreased processing time that increases output.

A study of thermal properties and thermal degradation kinetics of orthonovolaks based on *m*-cresol–formaldehyde (MCF) was conducted and related to PF orthonovolaks of similar compositions. Specific features emerge that can be related to the effect of methyl substitution on molecular weight, softening temperature, degradation profile, kinetics of degradation, etc.[4]

In the present investigation, we report the synthesis of a number of α-naphthol–formaldehyde (ANF) orthonovolaks. Here, the naphthalene ring is treated as an *ortho, meta* disubstitution (ring fusion) on the benzene nucleus. The consequence of resin composition on the softening temperature, 10 and 25% degradation temperatures (10% DT and

NCL Communication No. 5265.
* To whom correspondence should be addressed.

Journal of Applied Polymer Science, Vol. 50, 685–692 (1993)
© 1993 John Wiley & Sons, Inc. CCC 0021-8995/93/040685-08

25% DT), and activation energy (E) of the thermal degradation are discussed. The performances of ANF resins are compared relative to PF orthonovolaks of similar compositions.

EXPERIMENTAL

Analytical reagent-grade α-naphthol, phenol, formalin, and oxalic acid were used as received. Formaldehyde concentration in formalin was estimated by the standard procedure. The phenol-to-formaldehyde mol ratio was varied in different reactions between 1.00 : 0.80 and 1.00 : 1.05. Oxalic acid was used as the catalyst. In the second array of experiments, α-naphthol was reacted with formaldehyde. The α-naphthol-to-formaldehyde mol ratio was varied between 1.00 : 0.50 and 1.00 : 1.05.

The polycondensations were conducted in 500 mL four-necked round-bottom flask at 90°C for 6 h with constant stirring. The unreacted monomers were distilled out at reduced pressure at elevated temperature to obtain the resin. The resins were dried in a desiccator over phosphorus pentoxide. The softening temperatures were estimated with sealed glass capillaries on a melting-point apparatus.

The thermal behavior of resins was studied in air using a Netzch STA-409 thermal analyzer. The approximate sample size was 20 mg. Resins were heated at the constant rate of 10°C/min. Thermograms were obtained in the temperature range of 25–900°C.

RESULTS AND DISCUSSION

In ANF reactions, one of the three possible substitution sites in the aromatic ring is blocked by ring fusion. One *ortho* and one *para* reaction site is available for chain growth. Softening temperatures of PF (four compositions) and ANF (six compositions) novolak resins are shown in Table I. The softening temperatures in both series increase with the formaldehyde mol fraction in the resins. The replacement of the benzene ring in PF resins with the naphthalene ring in ANF resins increases the softening temperature an average of 50–60°C.

The thermal degradation of four PF resins and six ANF resins was examined. The superimposed plots of the rate of change in the mass of ANF resins in the temperature range 100–900°C are presented in Figure 1. Similarly, plots of PF orthonovolak resins in the temperature range 200–700°C are shown in Figure 2. The data on PF resins are used here for comparative study.

ANF resins are thermally stable to 200°C. The replacement of the benzene ring, in PF resins, with the naphthalene ring, in ANF resins, reduced the thermal stability considerably. The initial degradation temperature (T_i), final degradation temperature (T_f), and the temperature range (ΔT) over which degradation is observed in ANF resin series, presented in Table I, are compared with the data obtained for PF resins of similar compositions. The initial degradation temperatures (T_i) of ANF resins are lowered, on average, by 150°C. However, the final

Table I Thermal Properties of the Synthesized PF and ANF Orthonovolak Resins

No.	Sample Code	HCHO Mol Ratio	Temperature (°C)					
			Softening	T_i	T_f	ΔT	10% DT	25% DT
1	PF 105	1.05	96–99	367.4	649.0	281.6	405.2	512.4
2	PF 100	1.00	87–90	324.1	664.4	340.3	391.8	483.7
3	PF 090	0.90	74–78	328.5	634.5	306.0	385.8	474.2
4	PF 080	0.80	62–66	246.5	645.1	398.6	316.5	413.8
5	ANF 105	1.05	150–153	186.4	822.3	635.9	350.3	501.1
6	ANF 100	1.00	145–148	161.6	844.8	683.2	368.2	570.3
7	ANF 090	0.90	137–140	161.6	844.8	683.2	390.7	559.1
8	ANF 080	0.80	122–125	174.3	831.5	657.2	363.7	565.9
9	ANF 060	0.60	94–97	173.6	844.6	671.0	319.7	425.3
10	ANF 050	0.50	—	162.0	849.6	687.6	303.7	408.7

T_i, initial degradation temperature; T_f, final degradation temperature; ΔT, temperature range over which degradation is observed; DT, degradation temperature; PF, phenol–formaldehyde series; ANF, α-naphthol-formaldehyde series.

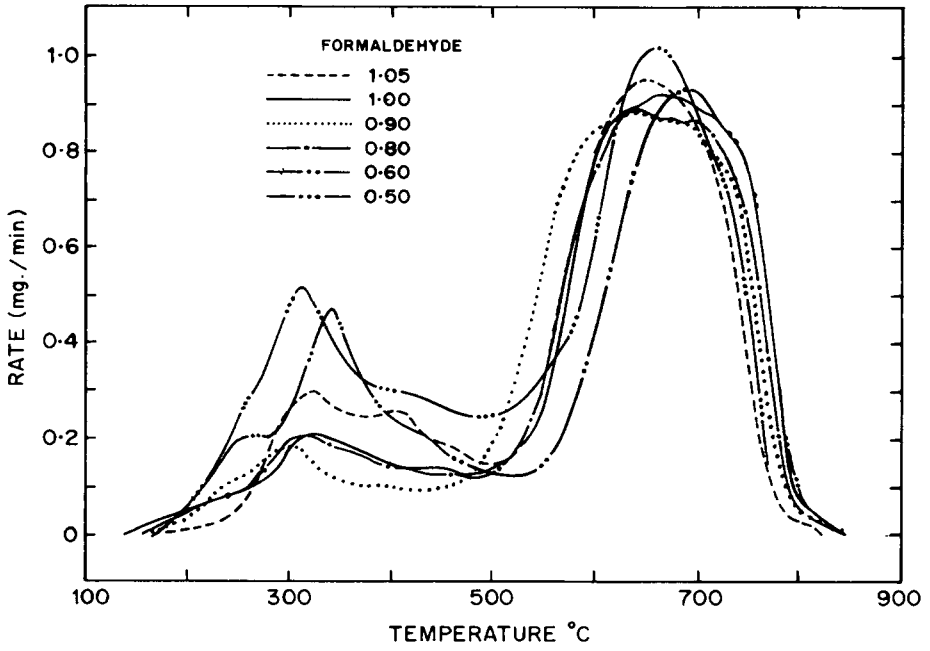

Figure 1 DTG thermograms for degradation of ANF resins at various compositions.

degradation temperatures (T_f) are higher and the temperature ranges (ΔT) over which degradation is observed are wider. The degradation temperature range (ΔT) in PF resins is around 300–400°C, whereas in ANF resins, it is around 650–700°C. This wide degradation range is probably due to the high melt viscosities of ANF resins, which would lower the rate of diffusion of the degradation products to the surface.

The data based on semiquantitative methods such as temperatures at 10 and 25% degradation (10% DT and 25% DT) are tabulated in Table I and are graphically represented in Figure 3. Three features that emerge are the following: (1) thermal stability

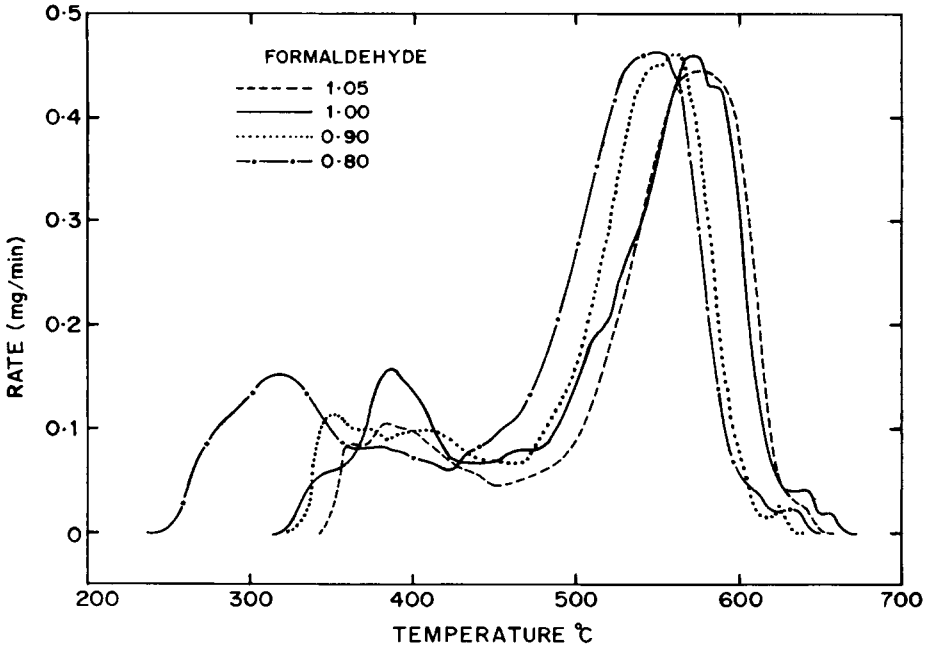

Figure 2 DTG thermograms for degradation of PF resins at various compositions.

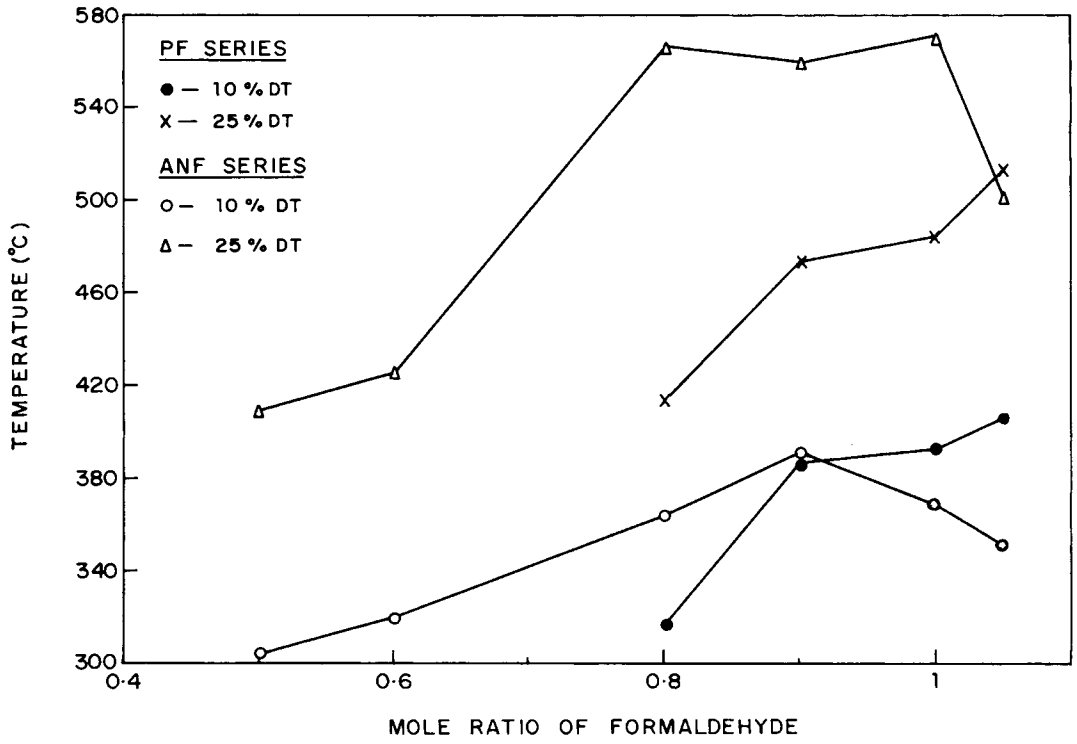

Figure 3 Plot of mol ratio of formaldehyde and decomposition temperature (10% *DT* and 25% *DT*).

of the ANF resin is lower than that of the PF resin of similar molar composition; (2) the degradation rate between 10 and 25% degradation is lower in ANF resins; and (3) the temperatures corresponding to 10 and 25% degradation decreases proportionally with the formaldehyde mol ratio in the resin.

The degradations occur in two distinct, initial and final, stages in both resin series, as seen in Figures 1 and 2. After an initial loss in mass, a rather sharp break occurred, indicating the onset of decomposition with rapid loss in the volatile fragments. The degradation in ANF resins starts around 150°C and is relatively rapid from 600°C. In the 150–500°C temperature range, corresponding to the initial degradation stage, the observed loss in mass is due to the volatilization of water and other lower molecular mass species.[5] The final degradation stage is observed after 500°C and is completed at around 800°C. Initial and final degradation stages of PF resins (Fig. 2) are observed in the temperature ranges 200–450°C and 500–600°C, respectively.

The final degradation stage is the predominant one in both resins. These are observable over similar temperature ranges irrespective of composition and chemical constituents.[6] This stage was selected for comparison of energy of activation (E) with respect to compositional and structural differences. The activation energies of the final degradation stage were evaluated. The DTG peak relating to this stage was separated out and corrected for area using the Anderson methodology.[7] The energy of activation (E) of the 10 resins were calculated from their DTG curves. Two nonisothermal integral methodologies were used to deduce the activation energies. The equations used are the following:

(A) Coats–Redfern Equation I (CR I)[8]:

$$\log\left[\frac{1-(1-\alpha)^{1-n}}{(1-n)T^2}\right] = \log\frac{AR}{aE}\left(1-\frac{2RT}{E}\right)-\frac{E}{2.303RT} \quad (1)$$

(B) Coats–Redfern Equation II (CR II):

$$\log\left[\frac{-\ln(1-\alpha)}{T^2}\right] = \log\frac{AR}{aE}\left(1-\frac{2RT}{E}\right)-\frac{E}{2.303RT} \quad (2)$$

(C) Horowitz–Metzger Method (HM)[9]:

$$\ln[-\ln(1-\alpha)] = E\theta/RT_S^2 \quad (3)$$

where $\alpha = (W - W_f)/(W_0 - W_f)$ (W_0, W_f, and W are the initial mass, final mass, and mass remaining at temperature T [equivalent to final degradation stage]), $\theta = T - T_S$, and T_S = the temperature at $W/W_0 = 1/e$. CR II is valid for reactions with order parameter (n) equal to 1 and CR I is applicable for reaction order parameters other than 1.

Order parameter n was evaluated using CR I and II. The plots of the left-hand-side function (LHS) vs. $1/T$ were drawn for different values of n in the range 0–3, excepting $n = 1$. CR II was used for $n = 1$. The superimposed plots of the LHS function in CR I or CR II vs. $1/T$ for the resin ANF060 are presented in Figure 4. For $n = 0$, 2, and 3 (CR I), a linear relationship was not observed, whereas for $n = 1$ (CR II), $\log[-\ln(1 - \alpha)]$ against $1/T$ was linear. This indicates that degradation in the last stage followed first-order kinetics. This was confirmed through Horowitz–Metzger (HM) equation.

The plot of $\log[\ln(1 - \alpha)^{-1}/T^2]$ vs. $1/T$ (CR II) and $\ln[-\ln(1 - \alpha)]$ vs. θ (HM equation) were plotted and the energy of activation (E) was evaluated from the slope of straight line for the 10 resin samples. The correlation coefficients "r" for the plots were also determined in each case. These were found to be near unity for the 20 plots, reflecting linearity of the curves.

Superimposed plots, for the second degradation stage of PF and ANF resins, of $\log[\ln(1 - \alpha)^{-1}/T^2]$ against $1/T$ (CR plots) are represented in Figures 5 and 6, respectively. The temperature ranges and extent of degradation within which analyses were conducted are represented in Table II. Here, the presented extent of degradation pertains only to that in the second degradation stage. Kinetic parameters for the 10 resins were analyzed in the 20–98% degradation range. The initial 20% degradation zone was bypassed to avoid errors due to an overlap from the previous degradation zone.[10] It is also known that in solids the initial stages' decomposition does not obey first-order kinetics.

Similarly, the superimposed plots of the second stage for PF and ANF resins, of $\ln[-\ln(1 - \alpha)]$ against θ (HM plots), are shown in Figures 7 and 8, respectively. Activation energies (E) calculated for these resins are tabulated in Table II. The activation energy (E) was computed from the slope of the Coats–Redfern and Horowitz–Metzger plots. A veritable trend was not discernible for activation energies (E) comparative to the formaldehyde content in these two orthonovolak series. This is most likely be due to variations in the molecular weights of the resins.[11] The number-average molecular weights of the PF and ANF resin series were estimated in acetone by vapor pressure osmometry. These were found to be in the ranges 1000–2500 and 1000–3700, respectively.[12]

The first-order reactions have an overall activation energy in the range of 150–200 kJ/mol for the PF resin series and 100–140 kJ/mol for the ANF

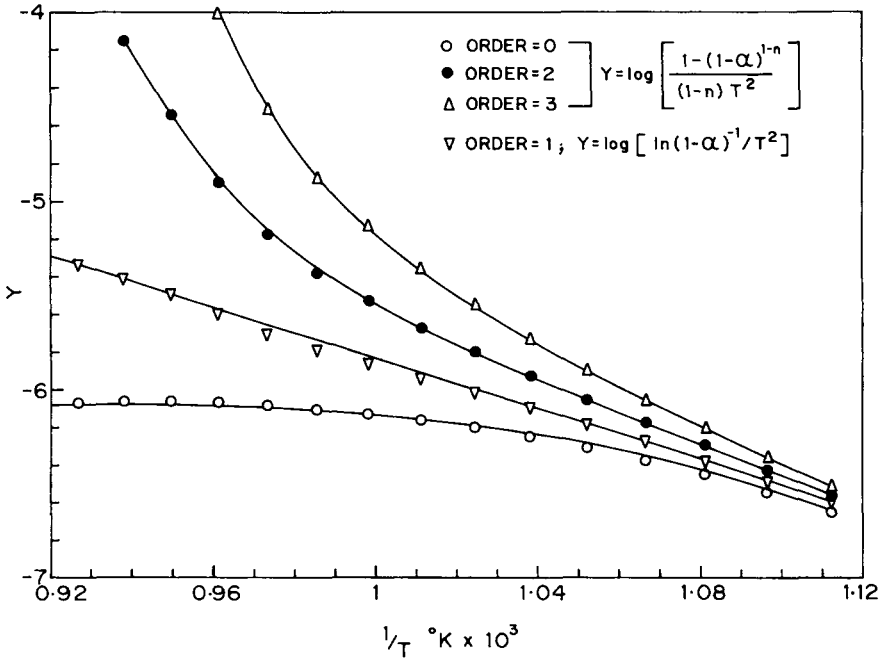

Figure 4 Coats–Redfern plots for ANF (1 : 0.6) resin at $n = 0$, 1, 2, and 3.

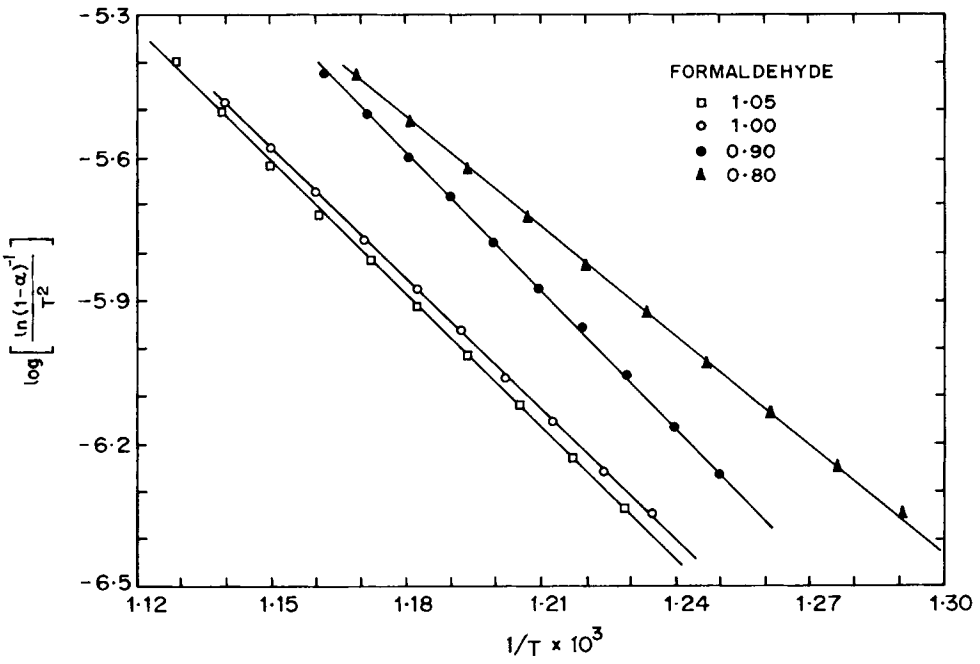

Figure 5 Coats–Redfern plots for PF resins at various compositions (last stage).

resin series. The activation energies (E) obtained from both Coats–Redfern and Horowitz–Metzger methods are tabulated in Table II. Higher values obtained by the Horowitz–Metzger method arise from the inexact approximation used in that derivation.[13] The activation energy of ANF resins are lower than that for PF resins.

Thermal degradation at higher temperature depends primarily on the stability of the dihydroxy diphenyl/dinaphthyl methane unit in phenol/ANF resins.[14] Ring fusion at *ortho* and *meta* positions of phenol resulted in a change in the chemical structure and stability of dihydroxy diphenyl methane unit. It has been reported that the thermal stability de-

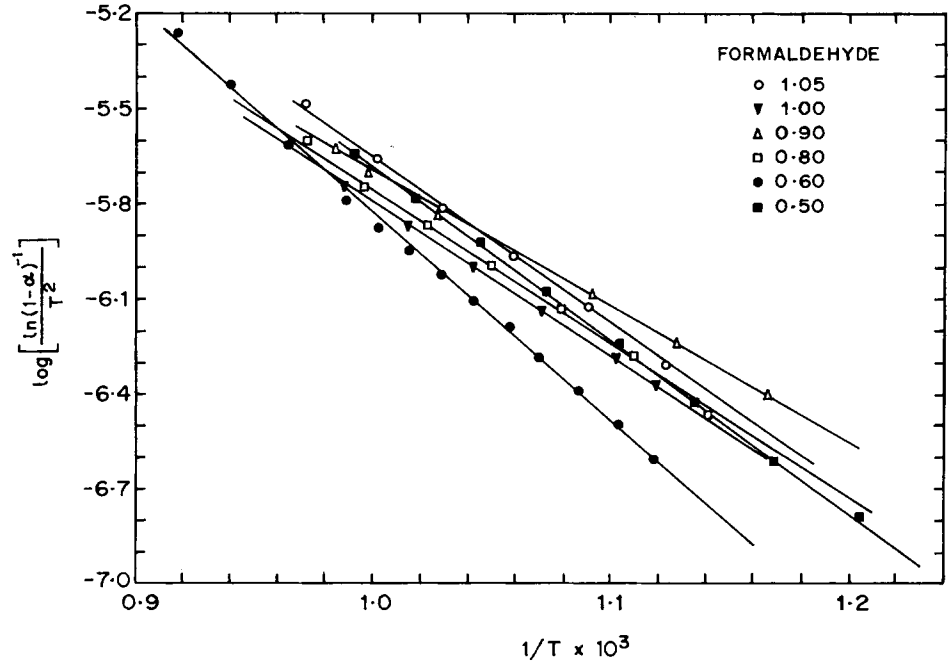

Figure 6 Coats–Redfern plots for ANF resins at various compositions (last stage).

Table II Decomposition Activation Energies in the Final Stage for PF and ANF Orthonovolak Resins

No.	Sample Code	HCHO Mol Ratio	Analysis Range: Temperature (°C) Start	Analysis Range: Temperature (°C) End	Analysis Range: Decomposition (%) Start	Analysis Range: Decomposition (%) End	Energy of Activation (in kJ/mol) HM	Energy of Activation (in kJ/mol) CR
1	PF 105	1.05	536.5	616.9	23.3	97.1	190.8	176.0
2	PF 100	1.00	532.8	611.7	22.5	94.8	188.2	172.4
3	PF 090	0.90	523.9	587.6	25.2	93.9	199.6	185.4
4	PF 080	0.80	497.5	582.5	20.4	93.4	162.6	146.1
5	ANF 105	1.05	617.2	781.3	31.6	99.4	117.9	107.0
6	ANF 100	1.00	621.7	805.5	28.7	99.8	113.3	100.3
7	ANF 090	0.90	585.6	787.2	24.8	99.0	99.6	85.1
8	ANF 080	0.80	603.6	793.5	22.9	99.3	114.5	100.1
9	ANF 060	0.60	620.6	818.2	17.9	99.8	137.9	123.8
10	ANF 050	0.50	608.6	760.8	24.7	97.8	123.5	106.0

HM, values obtained by Horowitz–Metzger method; CR, values obtained by Coats–Redfern method; PF, phenol–formaldehyde series; ANF, α-naphthol-formaldehyde series.

creases with an increase in molecular weight of substituted phenols.[6] Cross-linking is not possible in *para*-substituted phenols due to reduction in number of reactive sites from 3 to 2. This reduction in the number of reactive sites results in the reduced thermal stability. Similarly, the α-naphthol system may be considered to be equivalent to *ortho–meta*-disubstituted phenol. In this case, the number of active positions of phenol has been reduced from 3 to 2. Therefore, cross-linking is not possible and reduction in thermal stability is to be anticipated.

Variation in *para*-substitution from tertiary octyl to dodecyl in PF resins result in 70–85°C reduction in the thermal stability, on the basis of 10% *DT*. In these resins, the number of active positions are reduced from 3 to 2. In *meta*-substituted PF resins, wherein substitution is not at an active position, a 35–95°C reduction in thermal stability was observed

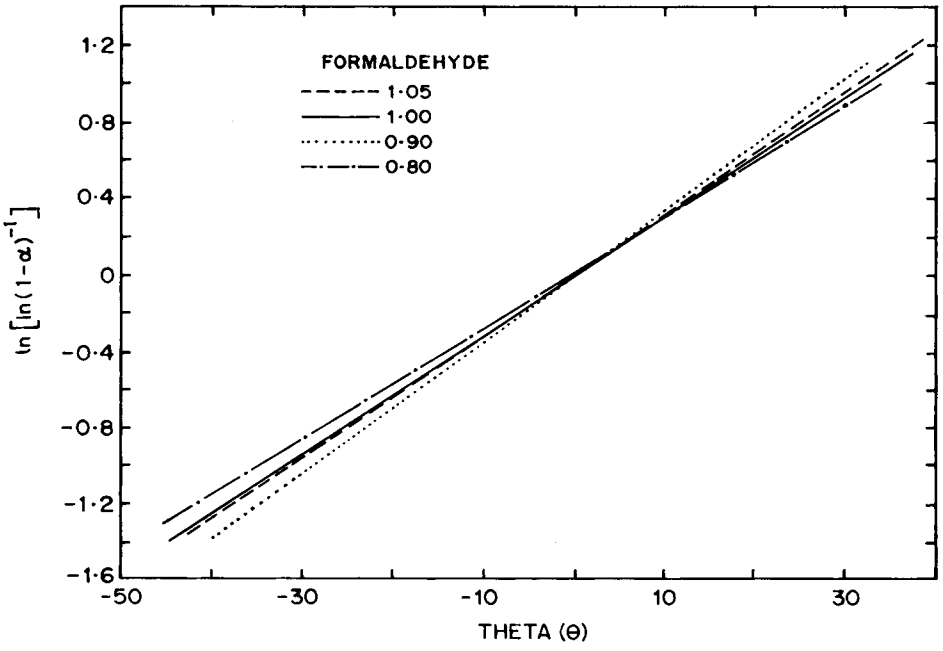

Figure 7 Horowitz–Metzger plots for PF at various compositions (last stage).

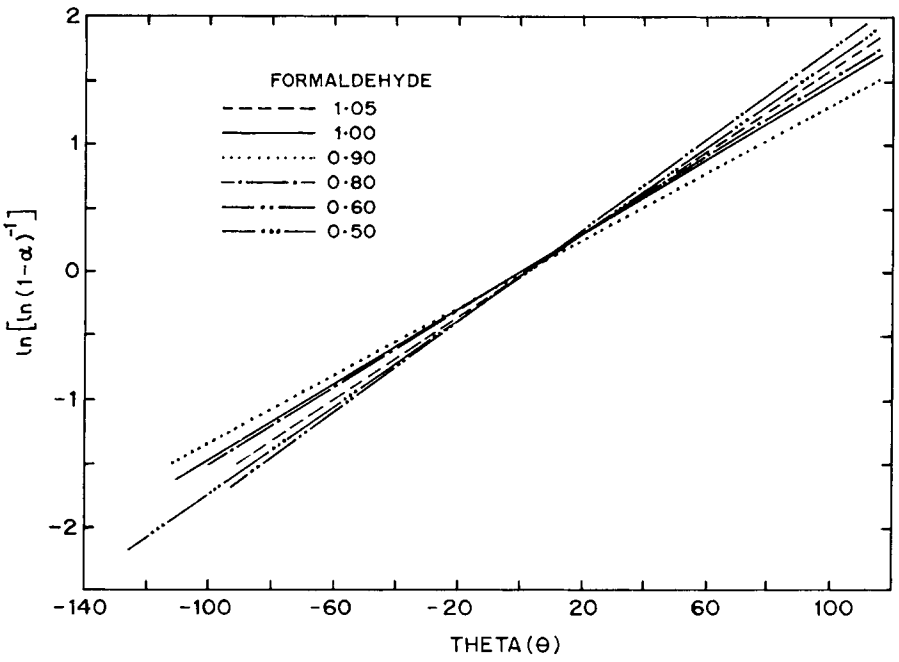

Figure 8 Horowitz–Metzger plots for ANF resins at various compositions (last stage).

by Jeffreys.[6] A similar trend was noted in *m*-cresol–formaldehyde orthonovolaks.[4] The overall activation energy for MCF (monosubstituted) orthonovolak resins was in the range 130–180 kJ/mol. This lies in between those observed for PF (unsubstituted) and ANF (disubstituted) orthonovolaks. Contributions arising from both these effects, namely, reduction in the number of active sites from 3 to 2 and substitution at nonactive sites, are noted in the α-naphthol ring (*o*–*m*-disubstituted phenol). Hence, a greater reduction in thermal stability in the ANF series is to be expected.

On the contrary, it is known that the stability of phenolic resins increase with the aromatic content in the resin network. Substitution in phenol reduces the thermal stability of PF resins, whereas increasing aromatic content increases the thermal stability. Hence, ANF resins 5 and 6 showed a lowering in the 10% *DT* temperature with respect to PF resins of similar composition. On the other hand, resins 7–10 showed an increase in 10% *DT* temperature. This increase in degradation temperature at 10% decomposition can be attributed to an increase in aromatic content with a decrease in the mol fraction of methylene bridges arising from formaldehyde. These two opposing effects, namely, substitution and aromatic content on thermal stability, are mutually nullified in the mol ratio 1.0 : 0.9 to 1.0 : 1.0 of α-naphthol and formaldehyde.

REFERENCES

1. F. A. Volenbrock and E. J. Spiert, *Adv. Polym. Sci.*, **84,** 85 (1988).
2. S. R. Turner and R. C. Daly, *J. Chem. Ed.*, **65,** 332 (1988).
3. A. Kumar, U. K. Phukan, A. K. Kulshrestha, and S. K. Gupta, *Polymer,* **23,** 215 (1982).
4. M. S. Chetan, R. S. Ghadage, C. R. Rajan, V. G. Gunjikar, and S. Ponrathnam, *Thermochim. Acta,* to appear.
5. M. Tugtepe and S. Ozgumus, *J. Appl. Polym. Sci.*, **39,** 83 (1990).
6. K. D. Jeffreys, *Br. Plast.*, **36,** 188 (1963).
7. D. A. Anderson and E. S. Freeman, *J. Appl. Polym. Sci.*, **1,** 192 (1959).
8. A. W. Coats and J. P. Redfern, *Nature,* **201,** 68 (1964).
9. H. H. Horowitz and G. Metzger, *Anal. Chem.*, **35,** 1464 (1963).
10. A. W. Coats and J. P. Redfern, *J. Polym. Sci. Part B,* **3,** 917 (1965).
11. B. V. Kokta, J. L. Valade, and W. N. Martin, *J. Appl. Polym. Sci.*, **17,** 1 (1973).
12. M. S. Chetan, B. Engg., Dissertation (1987).
13. C. G. R. Nair and K. N. Ninan, *Thermochim. Acta,* **23,** 161 (1978).
14. R. T. Conley, H. W. Lochte, and E. L. Strauss, *J. Appl. Polym. Sci.*, **9,** 2799 (1965).

Received November 2, 1992
Accepted January 17, 1993